SUPPLEMENTAL DATA

Description of the Comprehensive Assessment of At-Risk Mental States (CAARMS)

The CAARMS is a semi-structured interview designed to identify individuals at-risk for psychotic disorders. In this study, we obtained information from the participant and from available medical records. Four sub-scales of the CAARMS are used to identify an at-risk participant. They are unusual thought content, perceptual abnormalities, non-bizarre ideas and disorganized speech. All symptoms must have occurred in the past year, and are rated on a scale of 0 to 6 on both intensity and frequency of occurrence. Functioning in the past year is measured on the Social and Occupational Functioning Assessment Scale (SOFAS) on a scale of 0 to 100.

Participants can be categorized as at-risk if they fulfill any one of the 3 criteria groups; (1) Vulnerable group: family history of psychosis in a first degree relative, or presence of schizotypal disorder in assessed participant, (2) presence of attenuated psychotic symptoms in the past year, (3) brief limited intermittent psychotic symptoms.

Details of working memory task

In the LTR condition, four different uppercase letters were presented for 0.5 seconds, followed by a delay of 3.0 seconds during which a fixation star was displayed. This was followed by the presentation of a lowercase probe letter for 1.5 seconds and another fixation star for an additional 0.5 seconds. Participants were instructed to remember the 4 uppercase letters, match them to the lowercase probe letter, and then signal a match or a non-match by pressing one of two response buttons. Half the probes matched the target letters.

Data Supplement for Yaakub et al. (doi: 10.1176/appi.ajp.2013.12081135)

In the PLUS condition, two different uppercase letters were presented, and participants were instructed to shift each letter forward alphabetically by 1 position and to remember the results. For example, if “B” and “J” were presented, participants had to remember “c” and “k” to be matched with the probe. Half the trials were matches. Stimulus presentation sequence and timing were identical to that used in the LTR condition, except that a plus sign replaced the fixation star in the delay periods to denote the PLUS condition. The PLUS2 condition was identical to the PLUS condition except that participants had to shift each letter forward alphabetically by 2 positions, and 2 plus signs were presented during the delay period to indicate the condition.

The control condition was designed to match the perceptual and motor elements of the actual task conditions. Four identical uppercase letters were presented for 0.5 seconds, followed by a delay of 0.3 seconds and then a lowercase probe that matched the target in half the trials. This was followed by a 3.2 second delay during which a fixation star was presented. Participants signaled a match or non-match by using one of two response buttons.

Prior to imaging, participants performed a practice session outside the scanner to familiarize themselves with the task and to ensure that instructions were understood. Each condition was presented in 22-second blocks. Each block consisted of four trials (5.5 seconds per trial). Each experimental run consisted of 10 control blocks alternating with 9 task blocks, with 3 blocks of each condition presented per run in random order. Participants were required to achieve an accuracy of at least 75% on both the LTR and Control conditions.

In the scanner, participants were presented with 3 runs of alternating blocks, each lasting 7 minutes and 10 seconds. Stimuli were projected onto a screen and

Data Supplement for Yaakub et al. (doi: 10.1176/appi.ajp.2013.12081135)

viewed by participants using a rear-view mirror. Participants responded by pressing buttons on a MR-compatible response box held in their right hand.

Details of fMRI data acquisition and pre-processing

Images were acquired on a 3T Siemens Tim Trio system (Siemens, Erlangen, Germany). T2*-weighted images were acquired using a gradient echo-planar imaging (EPI) sequence (TR = 2000ms, TE = 30ms, FA = 90°, FOV = 192 192 mm, matrix size = 64 64 pixels). Twenty-eight oblique axial slices (4 mm thick with a 0.4 mm inter-slice gap) parallel to the anterior commissure-posterior commissure line were acquired. A high-resolution coplanar T1-weighted anatomical image was also acquired for image registration. An additional high-resolution anatomical reference image was acquired using a T1-weighted 3D multi-echo magnetization-prepared rapid-acquisition gradient echo sequence (TR = 2530 ms, TI = 1200 ms, FA = 7°, BW = 651 Hz/pixel, FOV = 256 256 mm, matrix size = 256 256 mm; resulting voxel dimensions = 1.0 1.0 1.0 mm) for the purpose of image display in Talairach space.

Intra-run motion correction was performed in-scanner and inter-run motion correction was performed using Brain Voyager QX version 1.10.4 (Brain Innovation), with each run realigned using rigid-body transformation to the first image of the functional run that was acquired closest in time to the coplanar T1-weighted image. Inter-slice timing differences attributable to slice acquisition order were adjusted using trilinear and sinc interpolation. Gaussian filtering was applied in the spatial domain by using a smoothing kernel of 8-mm full-width at half-maximum for group-level activation maps. A high-pass temporal filter (3 cycles) was also applied. The coplanar axial T1-weighted images were used to register the functional data set to

Data Supplement for Yaakub et al. (doi: 10.1176/appi.ajp.2013.12081135)

the high-resolution 3D image and the resulting aligned images were transformed into Talairach space.

Details of statistical analyses

Group-level analyses were conducted by using a random-effects model with subject as the random effect and task level as the fixed effect. Statistical t-maps were computed from a general linear model with a single predictor for each task condition (LTR, PLUS and PLUS2) by using separate subject predictors. Each predictor was represented by a boxcar function and convolved with a canonical hemodynamic response function. Three functional runs were included per participant. To account for baseline drifts across runs, z-transformation of the signal time-course for each run was performed. Task-induced activation against baseline was assessed using a voxel-level Bonferroni corrected threshold of $p<0.0001$.

A 3-condition by 2-group mixed-effects ANCOVA, with age, gender, education, handedness, ethnicity, and accuracy as covariates was computed to assess the main effect of group and condition-by-group interactions. A voxel-level threshold of $p<0.001$ (uncorrected) was applied to the resulting F-maps. To control for Type I errors, voxels surpassing the initial threshold underwent an iterative cluster thresholding procedure that considered the spatial smoothness of the data (1) to compute a spatial map based on a corrected cluster threshold ($p<0.05$). The significant clusters were masked using a binary mask of all task-related activations and deactivations thresholded at $p<0.0001$ (Bonferroni corrected).

We identified activation associated with the manipulation component by first contrasting each maintenance plus manipulation condition (PLUS and PLUS2) against the maintenance only condition (LTR) across both groups. The PLUS vs. LTR and PLUS2 vs. LTR contrasts were combined in a conjunction analysis

Data Supplement for Yaakub et al. (doi: 10.1176/appi.ajp.2013.12081135)

(thresholded at $p<0.0001$, Bonferroni corrected) for increased power. From the resulting conjunction map, 6 fronto-parietal regions known to be involved in working memory processes were selected as regions of interest (ROIs) to be considered for between-group analyses. ROIs consisted of voxels enclosed by a bounding cube of edge length 10mm surrounding an activation peak of interest.

For brain regions showing group differences in overall task-related activation, correlations between brain activity and clinical symptom severity or measures of cognition were calculated by correlating the average beta coefficient of the general linear model (GLM) for each task condition within the region of interest with the clinical or cognitive measures. Correlations between brain activity and clinical or cognitive measures in brain regions showing group differences in the manipulation of working memory contents were calculated by correlating the mean difference in beta coefficients of each manipulation condition and the maintenance only condition (PLUS–LTR and PLUS2–LTR) within the region of interest with the clinical or cognitive measures.

Effect of education on imaging results

Although the at-risk and control groups were not matched on education, there were no regions where the effect of the education covariate was significant at $p<0.001$; cluster level threshold $p<0.05$.

Data Supplement for Yaakub et al. (doi: 10.1176/appi.ajp.2013.12081135)

Subgroup analysis: comparison between the Vulnerable-Only participants (Subgroup 1, n=10) and those with psychotic-spectrum symptoms (Subgroups 2 & 3, n=42)

As it is important to understand subgroups within the at-risk population and to determine if there are any differences in brain activity between the subgroups, we compared activation in at-risk participants in the Vulnerable-Only participants (Subgroup 1) with those that show psychotic-spectrum symptoms (Subgroups 2 & 3).

There were no significant effects of group in either the **left insula** (Talairach coordinates: -24, 20, 13; $F_{(1,50)}$=0.14; n.s.) or the **posterior cingulate cortex** (Talairach coordinates: -3, -62, 31; $F_{(1,50)}$=2.01; p=n.s.). The parameter estimates across these regions are shown in Figure SF2A. There were no regions significant for condition-by-subgroup interactions.

Among the manipulation-related regions identified for the region of interest (ROI) analysis, the **right dorsolateral prefrontal cortex** ROI showed no significant task-by-subgroup interactions ($F_{(2,100)}$=0.47; n.s.; Figure SF2B).

There were no significant differences in brain activity between the two subgroups of at-risk participants. The graphs show trends that could be due to higher variability of parameter estimates in the smaller subgroup (Group 1, n=10).

Data Supplement for Yaakub et al. (doi: 10.1176/appi.ajp.2013.12081135)

Figure SF1. Plots comparing MR signal change for the Vulnerable Subgroup (n=10), Psychotic-Spectrum Symptoms Subgroup (n=42) and the Control group (n=38) in the A) left insula, B) posterior cingulate cortex and C) right dorsolateral prefrontal cortex ROI. Plots show the standard error of mean to illustrate higher variability of parameter estimates in the Vulnerable Subgroup. The MR signal change for the control group in each region is shown for comparison. D) The correlation between MR signal change associated with manipulation in the right dorsolateral PFC and PANSS total symptom scores in the at-risk group (r=0.40, p=0.001).

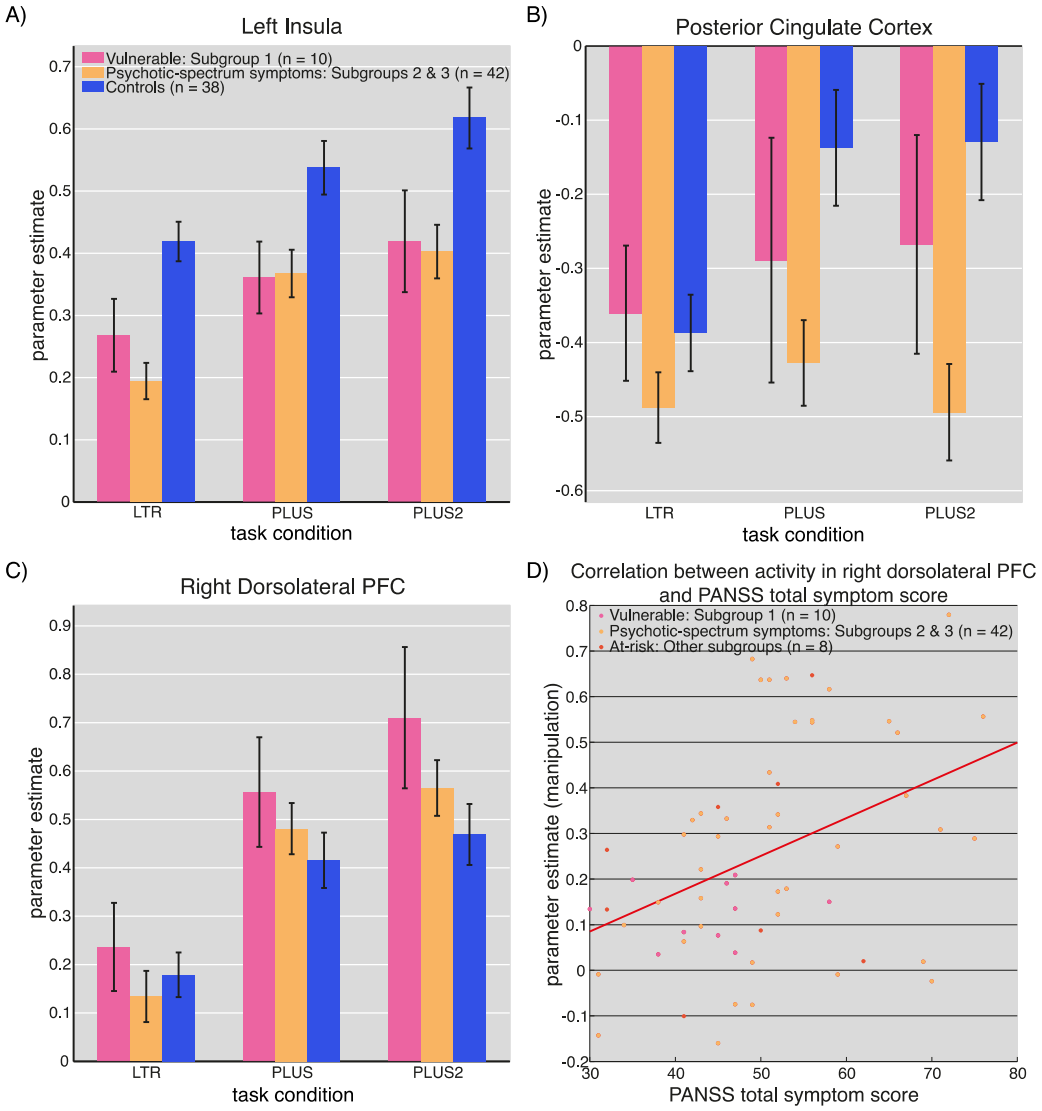

Data Supplement for Yaakub et al. (doi: 10.1176/appi.ajp.2013.12081135)

TABLE ST1. Location of activation peaks showing the main effect of group and condition-by-group interactions from whole-brain 3-condition by 2-group ANCOVAs and location of peaks of manipulation-related regions of interest (ROIs) derived from the conjunction of manipulation contrasts

Region	Talairach Coordinates			Analysis	
	x	y	z	ANCOVA (F)	p value
ANCOVA: Main effect of group					
Left anterior insula	-24	20	13	17.6	0.0001
Posterior cingulate cortex	-3	-62	31	14.5	0.0003
ANCOVA: Condition-by-group interaction					
Left middle frontal gyrus	-21	23	49	14.8	0.0000
Medial prefrontal cortex	-12	57	7	11.0	0.0000
Posterior cingulate cortex	-9	-49	22	9.7	0.0001
Right posterior insula	30	11	7	9.5	0.0001
Right inferior frontal gyrus	48	-4	22	9.4	0.0001
Left anterior middle frontal gyrus	-39	35	-5	9.4	0.0001
Right frontal eye field 1	33	-4	49	9.3	0.0001
Left precentral gyrus	-54	2	10	9.2	0.0002
Right frontal eye field 2	33	-4	49	8.7	0.0003
Precuneus	-3	-61	31	8.6	0.0003
	x	y	z	Analysis (t)[a]	
Manipulation-related ROIs					
Left dorsolateral prefrontal cortex (anterior)	-42	20	28	18.81	
Left inferior parietal lobule	-36	-49	37	17.56	
Left dorsolateral prefrontal cortex (posterior)	-45	5	34	16.72	
Right inferior parietal lobule	33	-61	37	13.68	
Right dorsolateral prefrontal cortex (posterior)	48	5	25	12.93	
Right dorsolateral prefrontal cortex (anterior)	45	26	34	11.75	

[a] Regional peak activation representing BOLD signal change that survived a threshold of $p<0.0001$, Bonferroni corrected.

Data Supplement for Yaakub et al. (doi: 10.1176/appi.ajp.2013.12081135)

Details of analysis and results with at-risk participants grouped according to antidepressant use

Table ST2. Behavioral performance of individuals with At-Risk Mental State who are medicated, ARMS non-medicated and Control participants

Behavioral Performance	At-risk Group (medicated) (n = 35)		At-risk Group (non-medicated) (n = 25)		Control Group (n = 38)	
	Mean	SD	Mean	SD	Mean	SD
Accuracy (%)						
LTR condition	90.1	8.8	92.9	7.7	91.5	8.3
PLUS condition	85.7	11.7	82.8	13.1	86.3	10.8
PLUS2 condition	78.2	15.2	78.4	16.2	81.1	14.5
Control condition	98.2	2.4	98.5	2.0	98.2	2.7
Reaction Time (ms)						
LTR condition	809.4	104.1	813.2	109.1	835.3	116.6
PLUS condition	864.2	148.9	885.7	153.2	885.4	168.3
PLUS2 condition	967.1	187.4	974.8	154.2	965.7	163.2
Control condition	612.0	90.5	608.6	88.4	605.7	103.8

Table ST3. Location of activation peaks showing a main effect of group and condition-by-group interactions from whole-brain ANCOVAs, taking into account medicated and non-medicated at-risk groups

Region	Talairach Coordinates			Analysis	
	x	y	z	F value	p value
ANCOVA: Main effect of group					
Left anterior insula	-24	20	13	8.8	0.0003
Posterior cingulate cortex	-3	-61	31	9.1	0.0003
ANCOVA: Condition-by-group interaction					
Left middle frontal gyrus	-21	23	49	7.9	0.0000
Precuneus	3	-43	46	6.6	0.0001
Left frontal eye field 2	-36	-7	46	6.3	0.0001
Medial prefrontal cortex	-12	59	21	6.6	0.0001
Right frontal eye field	30	-13	40	6.1	0.0001
Left frontal eye field 1	-21	-16	52	5.8	0.0002

Data Supplement for Yaakub et al. (doi: 10.1176/appi.ajp.2013.12081135)

Figure SF2. Plots comparing MR signal change for medicated vs non-medicated at-risk subgroups in regions where there was a main effect of group in the A) left insula and B) posterior cingulate cortex. C) Plot comparing MR signal change for medicated vs non-medicated at-risk subgroups in the right dorsolateral PFC region of interest, which showed a condition-by-group interaction.

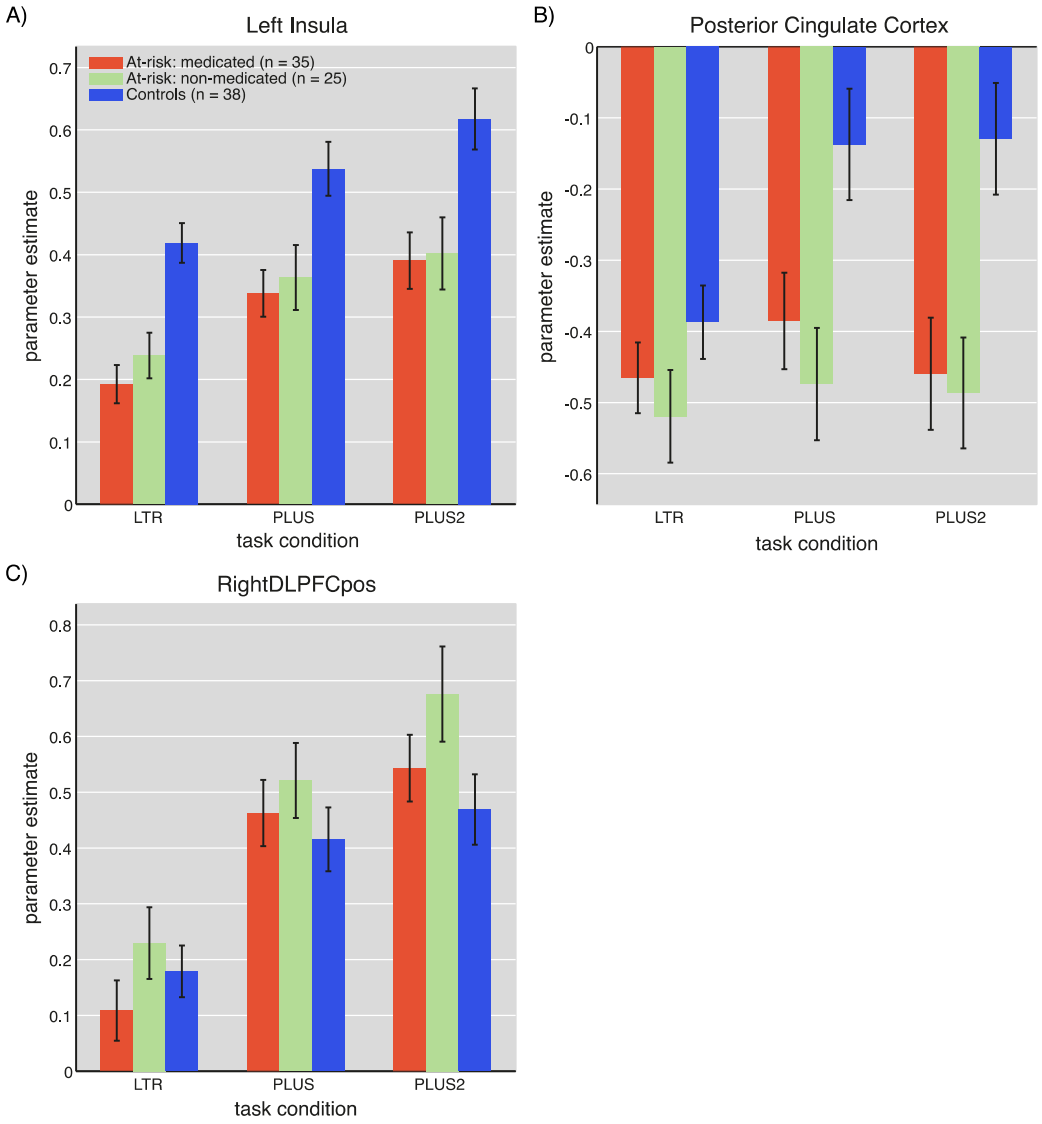

Data Supplement for Yaakub et al. (doi: 10.1176/appi.ajp.2013.12081135)

Comparison between participants who converted to psychosis (n=6) and those who did not convert to psychosis (n=54)

We compared participants who converted to psychosis (n=6) and those who did not convert (n=54) over a 2-year period for earliest recruits to a 1-year period for later recruits.

There were no significant effects of group in either the **left insula** (Talairach coordinates: -24, 20, 13; $F_{(1,58)}$=0.01; n.s.) or the **posterior cingulate cortex** (Talairach coordinates: -3, -62, 31; $F_{(1,58)}$=0.39; n.s.). The parameter estimates across these regions are shown in Figure SF3A. There were no regions significant for condition-by-group interactions.

Among the manipulation-related regions identified for the region of interest (ROI) analysis, the **right dorsolateral prefrontal cortex** ROI showed no significant task-by-group interactions ($F_{(2,116)}$=0.29; n.s.; Figure SF3B).

There were no significant differences in brain activity between the converted and non-converted at-risk participants.

Data Supplement for Yaakub et al. (doi: 10.1176/appi.ajp.2013.12081135)

Figure SF3. Plots comparing MR signal change for at-risk participants who converted to psychosis (n=6), those who did not convert to psychosis (n=54) over a minimum of 1-year follow-up period and the Control group (n=38) in the A) left insula, B) posterior cingulate cortex and C) right dorsolateral prefrontal cortex ROI. Plots show the standard error of mean to illustrate higher variability of parameter estimates in the group that converted to psychosis. The MR signal change for the control group in each region is shown for comparison.

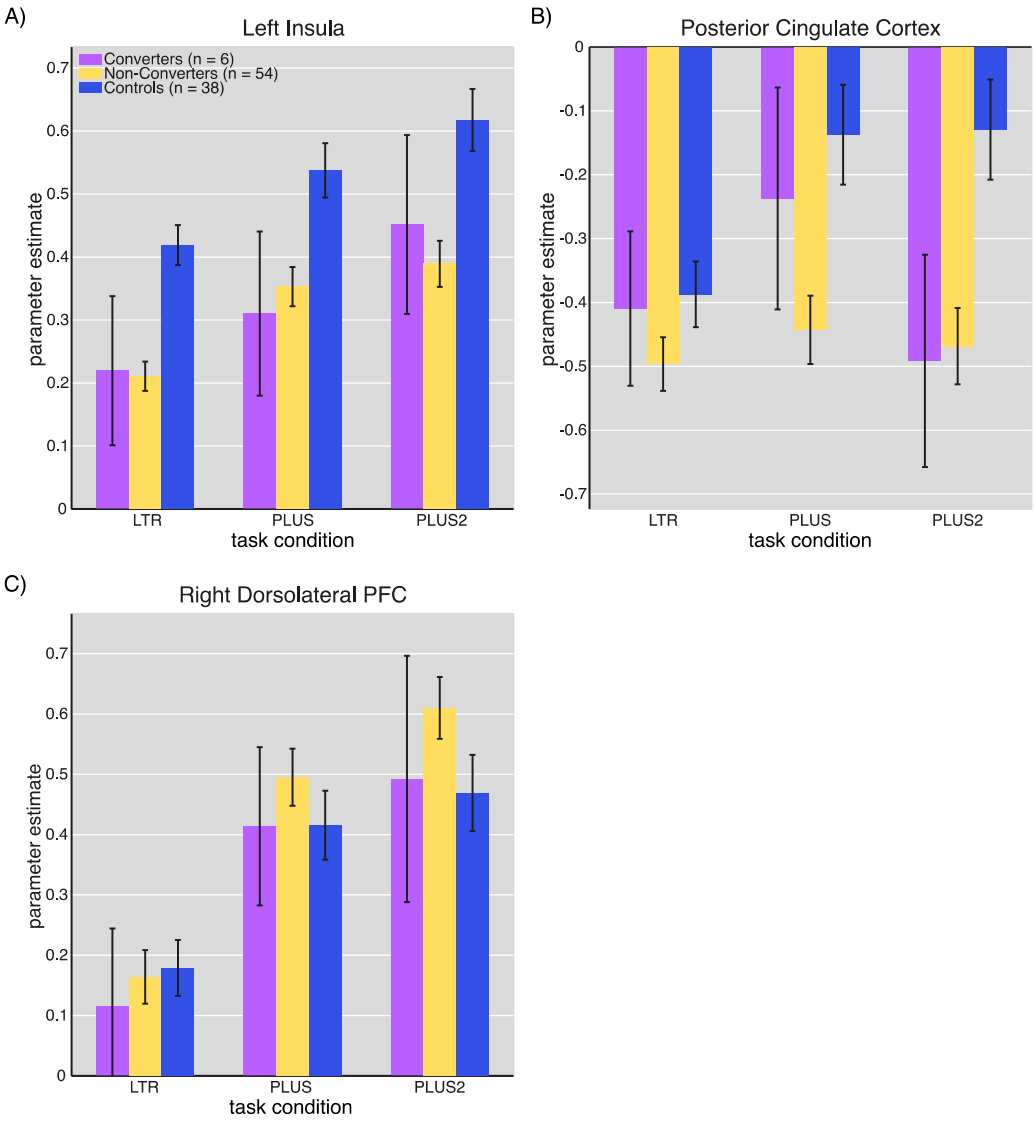

Data Supplement for Yaakub et al. (doi: 10.1176/appi.ajp.2013.12081135)

References

1. Goebel R, Esposito F, Formisano E: Analysis of functional image analysis contest (FIAC) data with brainvoyager QX: From single-subject to cortically aligned group general linear model analysis and self-organizing group independent component analysis. Hum Brain Mapp 2006; 27:392-401

Data Supplement for Yaakub et al. (doi: 10.1176/appi.ajp.2013.12081135)